Content-Aware Dark Image Enhancement through Channel Division

Adin Ramirez Rivera, Byungyong Ryu and Oksam Chae*, *Member, IEEE*

***Abstract*—Current contrast enhancement algorithms occasionally result in artifacts, over-enhancement, and unnatural effects in the processed images. These drawbacks increase for images taken under poor illumination conditions. In this paper, we propose a content-aware algorithm that enhances dark images, sharpens edges, reveals details in textured regions, and preserves the smoothness of flat regions. The algorithm produces an *ad hoc* transformation for each image, adapting the mapping functions to each image's characteristics to produce the maximum enhancement. We analyze the contrast of the image in the boundary and textured regions, and group the information with common characteristics. These groups model the relations within the image, from which we extract the transformation functions. The results are then adaptively mixed, by considering the human vision system characteristics, to boost the details in the image. Results show that the algorithm can automatically process a wide range of images—*e.g.*, mixed shadow and bright areas, outdoor and indoor lighting, and face images—without introducing artifacts, which is an improvement over many existing methods.**

***Index Terms*—Contrast enhancement, channel division, dark image enhancement, contrast pair**

EDICS Category: TEC-RST

I. Introduction

Contrast enhancement is essential to improve substandard images that are captured in extreme lighting conditions, such as excessively bright or dark environments that produce low contrast images, or are backlit, which produces normal global-contrast images with a low dynamic range in shadowed areas. Several algorithms have been proposed to overcome this problem: one of the simplest and most widely-used techniques is Histogram Equalization (HE) [1]. In HE, the cumulative density function (CDF) of the histogram is used as the intensity transfer function; this method enhances the contrast by distributing the CDF across the entire dynamic range. However, this even distribution creates artifacts in the smooth regions of the image. Moreover, it does not consider the boundaries, which degrades the sharpness of the resulting image.

Figure 1a presents a dark image, and Fig. 2a shows its histogram, which exhibits high accumulation in the dark intensities. Figure 1b is the result after HE; note the artifacts in the brighter regions of the image because a wider dynamic range was assigned to the dark areas in the histogram due to their dominance. This assignment expanded the dark regions and compressed the bright ones, which created artifacts. Another disadvantage of HE is the wash-out effect that occurs when the original histogram does not occupy the entire dynamic range of the image. Consequently, the equal redistribution of HE can leave gaps in the final histogram. Thus, several methods based on HE have been proposed in order to eliminate the shortcomings of the original technique [2]–[5]. For example, the Bi-Histogram Equalization (BHE) method [2], [5] splits the histogram into two parts based on where the mean lies. Each part is then enhanced independently using HE. BHE maintains the intensity mean of the original image, which suppresses the over-enhancement problem. Unnatural images are, however, still produced. Another popular method is Adaptive Histogram Equalization (AHE) [3], [4], whereby the histogram is equalized based on localized data. Even though AHE provides significant contrast enhancement and may preserve small details, over-enhancement and unnatural images are still occasionally produced. Contrast stretching algorithms and their adaptive versions (similar to AHE) are additional types of methods that can produce good results in dark images [6]; however, they produce no noticeable improvement if the image already occupies the entire dynamic range.

Consequently, researchers have developed more complex methods to overcome the limitations of previous methods. For instance, Safonov *et al.* [7] presented an enhancement

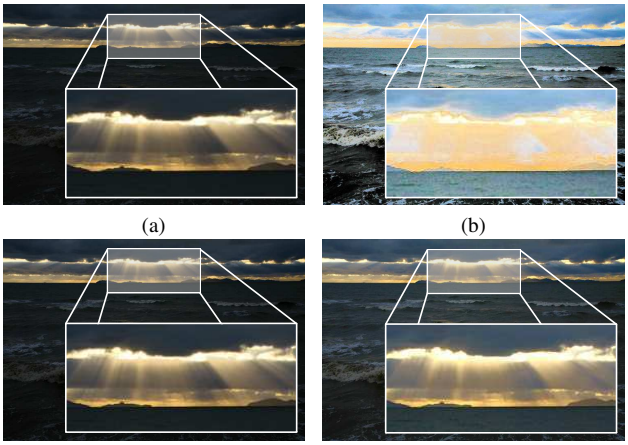

Fig. 1. Various enhancement techniques for a dark image. (a) Original image. (b) Result after HE, with artifacts. (c) Result of ORMIT, with minor enhancements. (d) Result of the proposed approach, revealing details without artifacts.

The authors are with the Department of Computer Engineering, Kyung Hee University, South Korea, 1 Seocheon-dong, Giheung-gu, Yongin-si, Gyeonggi-do 446-701.

* Corresponding author

e-mails {adin, read100nm, oschae}@khu.ac.kr

This work was supported by the National Research Foundation of Korea (NRF) grant funded by the Korea government (MEST) (No. 2012-0005523).

Manuscript accepted April 18, 2012.

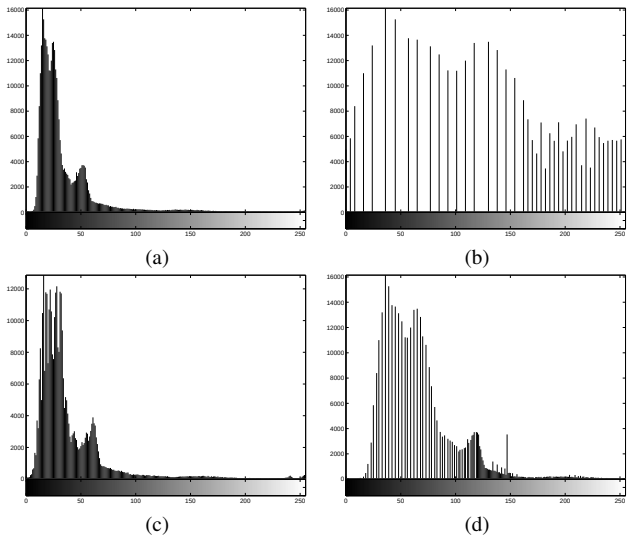

Fig. 2. Histograms of Fig. 1 (Gray level vs. Number of pixels). (a) Histogram of the dark image, with high accumulation in the dark intensities. (b) Histogram of the HE result, which is spread equally, thereby creating artifacts in the bright intensities. (c) Histogram of ORMIT result, which shows no spread in the dark intensities. (d) Histogram of the result using the proposed method, where the dark intensities are spread and the shape is maintained, which reduces the artifacts.

method based on contrast stretching and alpha-blending of both the brightness of the initial image and the estimations of reflectance. It used bilateral filtering to estimate and correct the reflectance of the image, while the brightness was corrected using alpha-blending. The method is, however, computationally expensive due to bilateral filtering, and it depends on several constants to work properly. Another complex method is the Multi-Scale Retinex (MSR) algorithm [8], which is a fast version of the Retinex algorithm proposed by Land [9]. Note that the proposal by Land [9] is a different version of the path-based Retinex [10]. The fast version of the MSR [8] is defined by

$$I_e = \sum_{n=1}^{N} (log(I) - log(LPF_n(I)), \tag{1}$$

where $LPF_n(\cdot)$ is the nth low-pass spatial filtering function (each with a different standard deviation), I is the image to be enhanced, I_e is the enhanced image, and N is the number of spatial filtering functions. Several other studies [11]–[14] have explored different versions of the MSR [8] in an effort to improve images; they performed a dark-tone correction based on variations of the MSR algorithm. Nevertheless, methods based on the MSR have high computational complexity. Another widely-used method is the image enhancement algorithm, Orthogonal Retino-Morphic Image Transform (ORMIT) [15], which is defined as follows:

$$I_e = \sum_{i=0}^{N} \alpha_i(I) \times LPF(P_i(F(I))) \times Q_i(F(I)) + \beta(I), \tag{2}$$

where $P_i(\cdot)$ is an orthogonal basis of functions defined in the range $(0, 1)$, $Q_i(\cdot)$ is an anti-derivative of $P_i(\cdot)$, $LPF(\cdot)$ is a low-pass spatial filtering operator, $F(\cdot)$ is a weighting function similar to gamma correction, N is the number of bands, $\alpha_i(\cdot)$ and $\beta_i(\cdot)$ are constants specific for each band, I is the image to be enhanced, and I_e is the enhanced image. The choice of appropriate $P_i(\cdot)$ functions allows the local contrast to be incremented. The use of a low-pass filter removes detail in the boundaries and produces a smooth variation in the sharp boundaries, which is an undesirable effect. The result of ORMIT applied to Fig. 1a (Fig. 1c) shows no noticeable improvement, and its histogram (Fig. 2c) does not shift the dark distribution to increase its dynamic range. These problems occur because the algorithm uses a pre-determined set of functions to transform the image, which is not ideal for all the different scenarios that exist. A solution to this problem is to use the content of the image to enhance it.

A first step in the content-based enhancement was the intensity pair distribution algorithm [16]. This algorithm combines the global properties of HE and the local properties of AHE. Both expansion and anti-expansion forces are used—the former models the intensity difference in the image, and the latter models the noise and intensity similarity. Moreover, the anti-expansion force is used as damping factor to compensate for the large accumulation in the expansion force. However, the accuracy of this reduction requires a manual adjustment in the algorithm parameters. Then, the transformation function can be generated by processing these forces. Yet, the accumulation of mixed forces (bright and dark intensities) in this algorithm leads to artifacts, and the method cannot handle sharp boundaries, although some modifications have been proposed [17], [18]. Furthermore, the intensity pair algorithm produces no noticeable improvement without specifically tuning its parameters.

In general, current enhancement algorithms use global information, which result in the creation of artifacts, such as halo-effects in sharp boundaries or noise effects. These algorithms also require significant computation time due to their complexity. Furthermore, they transform the image by using predefined functions that cannot anticipate all possible scenarios, and current methods employ smoothing functions that remove the sharpness from the resulting image. Additionally, these methods increase the contrast of flat regions, introducing artifacts and creating odd-looking images. To overcome all these problems, we analyze the content of the image and determine the transformation function based on the results of that analysis.

Given that humans have difficulty distinguishing the details in the dark areas of an image, especially compared to the mid and bright areas, our goal is to enhance the dark areas of the image without introducing artifacts. Unfortunately, this is a challenging task because the dark and bright regions need to be treated independently, and each image has different combinations of those regions. Thus, assigning a fixed dynamic range to each region will lead to undesired effects. Consequently, we propose a content-aware method that analyzes the contrast in the boundaries and in the texture regions to produce *ad hoc* transformation functions. We separate the different characteristics of the image and then group them by simulating the human visual characteristics. Due to the independent treatment needed for the groups, we build specific functions for each group that will enhance its characteristics.

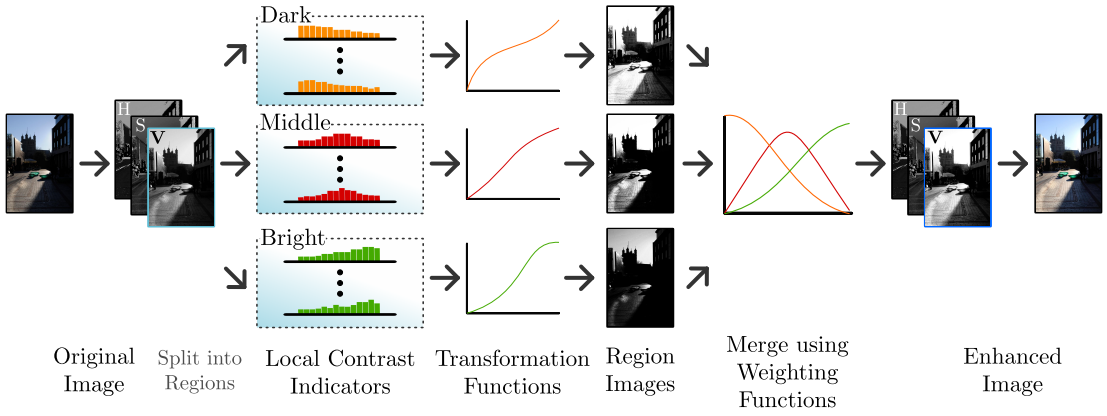

Fig. 3. An abstraction of the proposed algorithm.

Finally, the results of the groups' transformations are mixed adaptively to boost the details in the image. Figure 1d shows the result of the proposed method applied to Fig. 1a, which exhibits a greater improvement in the mixed regions (dark and bright) compared to the other methods. This improvement is due to the particular transformation function that was created through the analysis of the image, which preserves the image characteristics while revealing the details. In addition, the histogram corresponding to the proposed method (Fig. 2d) demonstrates that characteristics of the image were indeed preserved. Rather than change the shape of the histogram (as HE does) or redistribute it poorly (as ORMIT does), the proposed method spreads the dynamic range of the dark intensities and maintains the shapes of their distributions.

This paper is organized as follows: Section II describes the method of using contrast pairs in the channel division, as well as the procedure to build the transformation functions. Section III presents an evaluation framework for the enhancement algorithm. Section IV presents results that illustrate the effectiveness of the method compared with previous research. Finally, Section V provides some concluding remarks.

II. Channel Division Enhancement

Unlike previous methods that use fixed transformation functions, the proposed algorithm builds an *ad hoc* transformation function based on information extracted from the image. That information comes from the contrast in the boundaries and the texture regions. Inspired by intensity pairs [16], we encode contrast using *contrast pairs*. These pairs model the contrast relation between the intensities of two neighboring pixels. In other words, consider that, in the enhancement process, each contrast pair acts like a force that spreads the intensities that define it. Hence, when many pixels that share similar characteristics (such as dark or bright intensities) are neighbors, the forces created by their contrast pairs will separate their intensities. Conversely, isolated pixels will maintain their intensities due to the lack of interaction. Thus, we accumulate the contrast-pairs into *local contrast indicator* (LCI) functions, and merge such functions into *channels*, to reduce the artifact creation—a process that we termed *channel division*. We introduce this process because the accumulation of mixed contrast-pairs inaccurately spread the dynamic range of some intensities, due to the contribution of intensities with different characteristics, such as bright intensities contributing to the separation of dark intensities. Then, we group the channels into *region channels*, which may simulate human visual characteristics, and create a set of transformation functions from their accumulated LCIs. Furthermore, we used a finer grain for the channel division—*i.e.*, *intensity channels*, that allow us to control the interference and overlap of the contrast pairs. These intensity channels became the building blocks for the region channels. Finally, we used the region channel functions to enhance the specific characteristics of each image, and we merge the results of that process to reduce the artifacts and to ensure maximum enhancement. Figure 3 summarizes the entire algorithm.

To implement the proposed algorithm, we first transform the image to the Hue-Saturation-Value (HSV) color space. Then, we apply the proposed algorithm to the image intensity (V component). After the enhancement, we use the hue (H) and saturation (S) components from the original image and merge them with the enhanced intensities to create the final image. This procedure maintains the color (HS) of the image while improving its intensity level (V).

Unlike previous intensity-pair based methods [16]–[18], we use a simplified expansion force, in the form of a LCI. Moreover, in our experiments, we found that the inclusion of the anti-expansion force, that models the intensity similarity (smoothness) of the image and that is used as a damping factor [16]–[18], produced no noticeable improvements to the enhanced image, thus we did not use it. Moreover, previous methods adjusted the transformation function by tuning the contributions of the expansion and anti-expansion forces manually. In contrast, our method uses the channel division and mixture process to adjust the final transformation, which thereby enhances the image. Furthermore, since our method uses a quadratic space in the number of intensities, our simpler LCI functions compensate for the complexity introduced by the channel division, especially compared to previous methods. In average, for a general image, of approximately 415 thousand pixels (665×625), our method needs 368 ms to enhance it. Specifically, images of 533×400 and 1000×664 pixels are processed in 163 ms and 583 ms. We compute these times

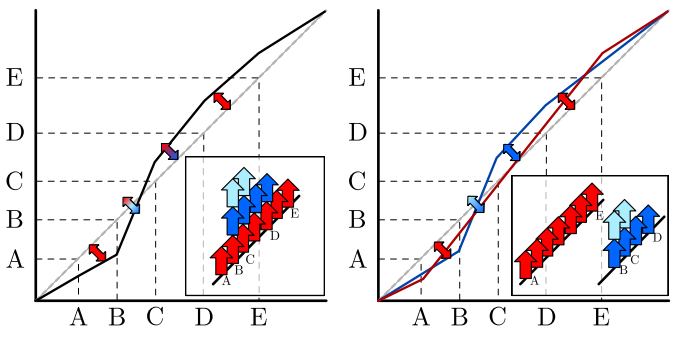

(a) Single channel (b) Multiple channels

Fig. 4. Different approaches to accumulate the votes of three contrast pairs, ρ_A^E, ρ_B^C and ρ_B^D. (a) A single channel accumulation of contrast pairs (as previous methods did) is divided into (b) two different channels. The accumulated contrast pairs are shown in the boxes, and their local contrast indicators (represented by the arrows) shift the identity function (in gray) into their transformation functions (shown in (a) black and (b) blue and red).

using a 4 GB RAM and 2.5 GHz dual-core computer, with un-optimized code written in C++.

A. Contrast Pair

We model the contrast—*i.e.*, the intensity difference between two pixels—in the image through contrast-pairs, which are similar to those proposed by Jen *et al.* [16]. A contrast pair acts like a force that spreads apart the intensities that define it. We model the interaction of the contrast pairs as a local contrast indicator function. Consequently, we define a contrast pair, ρ_i^j, between two given intensities, i and j, as a set of votes for every intensity in the intensity set $\{i, \ldots, j\}$. Moreover, we can consider the contrast pair, ρ_i^j, to be a vector of intensities whose length is equal to the intensities that has ones (votes) in the set $\{i, \ldots, j\}$ and zeros anywhere else, similar to the vectors shown in Fig. 4. Spatially, the contrast pairs are constructed from the image using the eight neighbors of each pixel. We define the set of contrast pairs for a pixel (x, y) as

$$P(x,y) = \{\rho_{I(x,y)}^{I(x',y')} \mid (x',y') \in \mathscr{N}(x,y)\}, \tag{3}$$

where $\rho_{I(x,y)}^{I(x',y')}$ is a contrast pair, $\mathscr{N}(x,y)$ contains the eight neighbors of (x,y), and $I(x,y)$ and $I(x',y')$ are the intensities of the pixels (x,y) and (x',y'), respectively. The contrast pairs can be computed efficiently by scanning the top-left neighbors of each pixel (*i.e.*, the three neighbors above the pixel and the one directly to its left), and the other four pairs are processed when the bottom-right neighbors are scanned. This process is possible because the contrast pairs are commutative—*i.e.*, $\rho_i^j = \rho_j^i$, and both define the same interval [16].

We classify the contrast pairs of each image into two classes: *edge* and *smooth*. The former is found in the boundaries and texture regions, while the latter is found in the flat regions. To classify the pairs, we take the intensity difference between the pair's intensities. If it exceeds some defined threshold ε (in our experiments we used 10 intensity levels), then it is considered an edge contrast pair; otherwise it is considered a smooth contrast pair.

To create the transformation functions, we use the LCI from the contrast pairs. Unlike Jen *et al.* [16], we use only the normalized LCI to compute the transformation function because we found that the channel division provides more enhancement than the proposed method by Jen *et al.* Consequently, the LCI in the proposed model is the accumulation of the votes defined by the contrast pairs. In addition, we focus on the edge contrast pairs because their accumulation determines the transformation needed to reveal the details of the image. As shown in Fig. 4, the LCI produce different slopes according to their accumulation. Hence, when there is a high accumulation of contrast pairs, a steep slope is generated in the transformation function, and the intensities are spread farther apart. In contrast, when there is a small accumulation, the slope is close to the identity function, which maintains the intensities throughout the transformation. This procedure also preserves the aspect of the flat regions by ignoring the contribution of the smooth contrast pairs in the transformation. Hence, those intensities are not separated, which maintains the appearance in the flat regions. As a result, the accumulation of all the edge contrast pairs generates an LCI function, $\boldsymbol{f}$, defined by

$$f(i) = \sum_{x,y} \sum_{\rho \in P_e(x,y)} \rho(i), \tag{4}$$

where $f(i)$ is the ith position of the LCI $\boldsymbol{f}$, which acts like a vector of the accumulated votes from the contrast pairs, x and y are coordinates of the image, $P_e(x,y)$ is the set of neighboring-edge contrast pairs for pixel (x,y), $\rho(i)$ is the ith position in an edge contrast pair of (x,y), i is the intensity index in the range $0 \leq i \leq N$, and N is the maximum number of intensities. Note that, for simplicity, the intensities have been removed from the contrast-pair notation for pairs that are identifiable. Furthermore, the edge contrast pairs for the pixel (x,y), $P_e(x,y)$, are defined by

$$\begin{aligned} P_e(x,y) = \{\rho_{I(x,y)}^{I(x',y')} \mid (x',y') \in \mathscr{N}(x,y) \\ \wedge |I(x,y) - I(x',y')| \geq \varepsilon\}, \end{aligned} \tag{5}$$

where (x,y) and (x',y') are positions of the pixels in the image with intensities $I(x,y)$ and $I(x',y')$, $\mathscr{N}(x,y)$ contains the eight neighbors of (x,y), and ε is a constant. Once the LCI is computed, it is integrated and normalized by

$$F(k) = \frac{\sum_{i=0}^{k} f(i)}{\sum_{i=0}^{N} f(i)}, \tag{6}$$

where $F(k)$ is the kth position in the integrated force $\boldsymbol{F}$, $f(i)$ is the ith position in the LCI $\boldsymbol{f}$, k is the intensity index in the range $0 \leq k \leq N$, and N is the maximum number of intensities.

Since the transformation function should be monotonically increasing and single valued [1], we normalize and project the transformation function $\boldsymbol{T}$ onto the identity transformation $\boldsymbol{I}$, which is defined by $I(x) = x/N$ for $0 \leq x \leq N$. Then the transformation function can be defined by

$$T(k) = \frac{I(k) + F(k)}{\max(\boldsymbol{I} + \boldsymbol{F})}, \quad 0 \leq k \leq N. \tag{7}$$

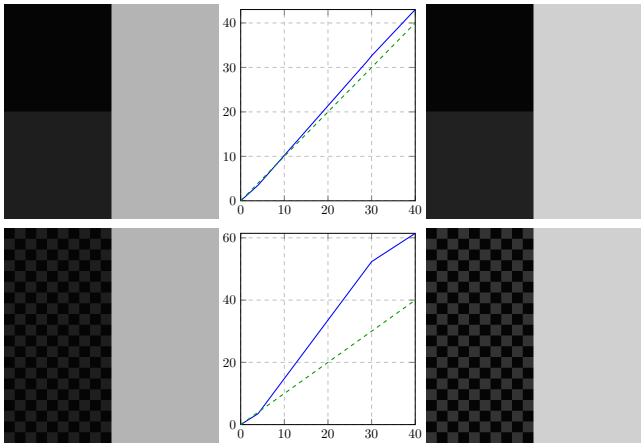

Fig. 5. Two (a) synthetic images, with same global contrast but different local contrast, produced different (b) transformations and (c) enhanced images. The top row, shows an image with few interaction between its intensities and few enhancement, while the bottom row shows high interaction between its intensities and high enhancement in comparison with the top row.

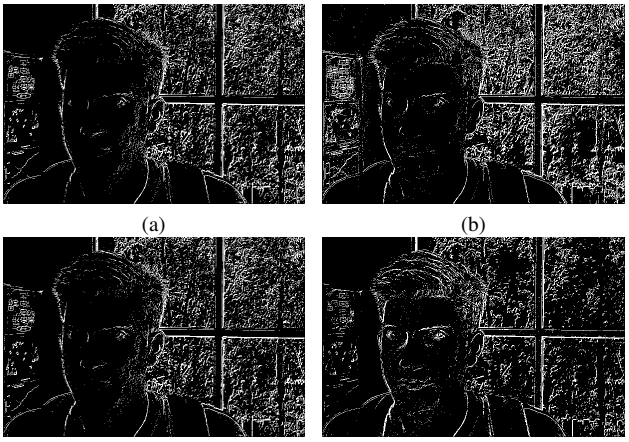

Fig. 6. Edge contrast pairs of (a) the original image, (b) the result of HE, (c) the result of ORMIT, and (d) the result of the proposed approach. The pairs reveal the level of detail exposed in each image.

B. Intensity Channels

As stated before, the contrast pairs may belong to different intensity regions. Thus, one accumulation of contrast pairs does not represents the intensity relations, and may separate the intensities that should stay together. To overcome this problem, we group the contrast pairs into *intensity channels*. Thereby, each contrast pair is accumulated into an intensity channel (LCI) that corresponds to each intensity, in order to isolate the contribution of the contrast pairs. Consequently, the transformations extracted from the intensity channels produce better results than a global transformation because the LCI of each channel affects only its peers. Hence, our proposed transformations avoid the incorporation of LCIs that excessively spread the intensities of the group, and consequently, compress other intensities. For instance, Fig. 5 shows two synthetic images with two different patterns and with the same global contrast but different local contrast. The first row shows a low local-contrast pattern, while the second row shows a high local-contrast pattern. After applying the channel division approach to both images, we can see that the second image produces a steeper transformation, in the range of the dark intensities (from 5 to 30 in Fig. 5b). Consequently, the steepness is translated into more enhancement as seen in the resultant images (as shown in Fig. 5c, the first-row transformation maps 30 to 33, while the second-row transformation maps it to 52; the other dark intensity is leave as is in both cases). Moreover, the bright intensity is equally enhanced in both cases (from 180 to 189) due to the equal number of pixels interacting in the boundary between the dark and bright intensities. Whereby, the local-neighborhood contrast affects the final transformation. Therefore, our algorithm maintains the flat regions in the image and enhances the textured regions, which avoids the introduction of artifacts.

To explore this phenomenon further, let ρ_A^E, ρ_B^C and ρ_B^D be three contrast pairs, with their respective set of votes cast in the intensity sets $\{A,\ldots,E\}$, $\{B,\ldots,C\}$, and $\{B,\ldots,D\}$, such that $A < B < C < D < E$. In the global accumulation approach, the three contrast pairs are accumulated into the same LCI, as shown in Fig. 4a. This process leads to over-enhancement problems and artifacts because the pairs of the intensity B (ρ_B^C and ρ_B^D) create a mixed LCI with the pairs of the intensity A (ρ_A^E). Therefore, the intensities A and E, which would be spread evenly, as shown in Fig. 4b, are spread farther apart due to the contribution of the B-pairs, although those pairs are unrelated to A and E. These errors can be avoided if each group's pairs are separated and each LCI is computed independently.

The creation of intensity channels enhances the contrast of one image's area without introducing artifacts. Previous methods, even those that use image information [16]–[18], fail to avoid artifacts because they use the image information without considering its intensity relations. Figure 6 shows the edge contrast pairs of a face image damaged by shadows. We can see that the shadows in the image hide the details in the face, as shown in Fig. 6a. Although other methods reveal some details of the scene, as shown in Figs. 6b and 6c, the face is not distinguishable. The proposed method, however, can recover these details, as shown in Fig. 6d. This distinction is due to the channel division approach, in which the pairs in the shadow areas force the intensities of those around them to spread apart without affecting other areas' intensities, unlike the HE result, which reveals more background details than face details due to its equal distribution characteristic.

The intensity channel LCI, $\boldsymbol{f}^i$, for the intensity i is defined by

$$f^i(j) = \sum_{x,y} \sum_{\rho \in P_e^i(x,y)} \rho(j), \tag{8}$$

where $f^i(j)$ is the jth position in the LCI $\boldsymbol{f}^i$, x and y are coordinates of the image, $P_e^i(x,y)$ is the set of the eight neighboring edge contrast pairs for the pixel (x,y) such that the intensity i is within that pair's intensity, and $\rho(j)$ is the jth position in an edge contrast pair of (x,y). Note that i and j vary from zero to the maximum number of intensity levels, N. Furthermore, the set of edge contrast pairs for the pixel

(a) (b) (c) (d)

Fig. 7. Enhancement produced by the channel division using different intensity region channels. (a) The original dark images. (b-d) The enhanced images showing specific characteristics (dark, mid, and bright tones): (b) dark, (c) middle, and (d) bright region channels.

(x, y) and intensity i, P_e^i, is defined by

$$P_e^i(p) = \{\rho_{I(x,y)}^{I(x',y')} \mid (x', y') \in \mathscr{N}(x, y) \wedge |I(x, y) - I(x', y')| \geq \varepsilon \wedge (i = I(x, y) \vee i = I(x', y'))\}, \quad (9)$$

where (x, y) and (x', y') are the positions of the pixels in the image with intensities $I(x, y)$ and $I(x', y')$, respectively, $\mathscr{N}(x, y)$ contains the eight neighbors of (x, y), and ε is a constant. Finally, the accumulation for each intensity channel LCI, $\boldsymbol{F}^i$, is computed as in Eq. (6), and their transformation functions, $\boldsymbol{T}^i$, are projected as in Eq. (7), by replacing $\boldsymbol{f}$ with $\boldsymbol{f}^i$ as follows:

$$F^i(k) = \frac{\sum_{j=0}^{k} f^i(j)}{\sum_{j=0}^{N} f^i(j)}, \quad (10)$$

$$T^i(k) = \frac{I(k) + F^i(k)}{\max(\boldsymbol{I} + \boldsymbol{F}^i)}, \quad 0 \leq k \leq N. \quad (11)$$

C. Region Channels

Grouping the contrast pairs into intensity channels is not sufficient to produce the best enhancement, as there may be (intensity) channels with similar properties. We propose to mix the channels with similar characteristics into *region channels*. Consequently, a region channel is a mix of intensity channels that share some characteristics. Hence, an image may have R different region channels that are defined by

$$\boldsymbol{T}_r = \frac{\sum_{i=I_{\min}^r}^{I_{\max}^r} \boldsymbol{T}^i}{I_{\max}^r - I_{\min}^r + 1}, 1 \leq r \leq R, \quad (12)$$

where $\boldsymbol{T}_r$ is the rth region channel transformation, $\boldsymbol{T}^i$ is the transformation function for each intensity channel i, and $I_{\min}^r$ and $I_{\max}^r$ are the lower and upper bound (intensities) for the rth region channel (the $(r-1)$st and the $(r+1)$st channel may share their upper and lower bounds with the rth channel).

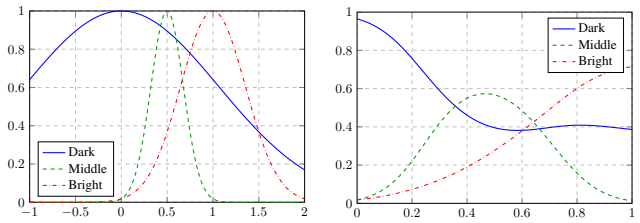

(a) Shifted Gaussians (b) Normalized Gaussians

Fig. 8. A set of weighting functions. We construct the weighting functions for the region channels from (a) a set of shifted Gaussians. The final functions are (b) those Gaussians normalized.

Experimentally, we found that mixing our intensity channels into three regions (R equal three), that may simulate the human visual system, further improves the resultant image. We approximate each region channel to accommodate dark, middle and bright intensities (which may be similar to the human visual system regions: De Vries-Rose, Weber and Saturation—despite previous research showed [19], [20] the viability of approximating the human visual response with three regions, for our channel division approach this possibility is yet to be proven in further research), respectively. Consequently, we build a transformation function for each region channel that will spread its intensities due to the interactions of that region's intensities. These functions produce different results, as shown in Fig. 7, which are then merged using weighting functions to create the final image. Because we are working with dark images, we give more importance to the dark intensities, compared to the other intensities, to boost the enhancement of the dark intensities without compromising the result of the other two region channels.

To illustrate the region channels, Fig. 7 presents dark images enhanced by the specially-constructed functions given in Eq. (12), which are defined by each region channel. Although the images are composed mostly of dark intensities, the image from the dark region channel (Fig. 7b) is enhanced more because of the abundance of dark intensities in that channel; thus, the interactions of these intensities lead to a greater contrast within the dark components of the image. Conversely, the components of the middle and bright region-channel images (Figs. 7c and 7d) are preserved because their contrast pairs accumulated a LCI that does not separate them, thereby avoiding over-enhancement in areas containing those intensities. These results also show the advantage of using multiple channels over a single channel approach. For instance, in the single channel approach, due to the mixed interaction of bright and dark pixels and the high interaction of the dark contrast pairs, the bright intensities will be separated by the LCI from the dark contrast pairs, which may generate artifacts.

As previously discussed, each region channel possesses different characteristics of the original image (see Fig. 7). Given that we are working with dark images, the dark region channel will be wider than normal and will have as many or more elements as the other two region channels. Consequently, we approximate the width of the each region channel to one-third of the intensity range. These values were determined experimentally to yield the most optimal results. Moreover,

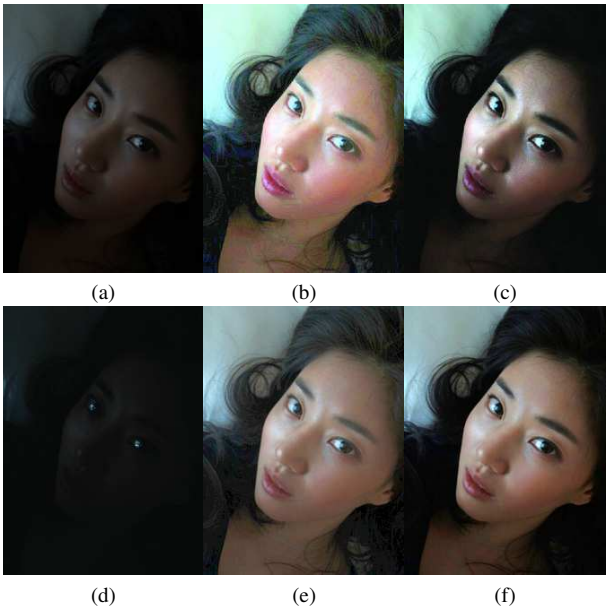

Fig. 9. Dark image: "Girl." (a) Original image, (b) HE result, (c) intensity pair result, (d) LRM result, (e) ORMIT result, and (f) proposed method result.

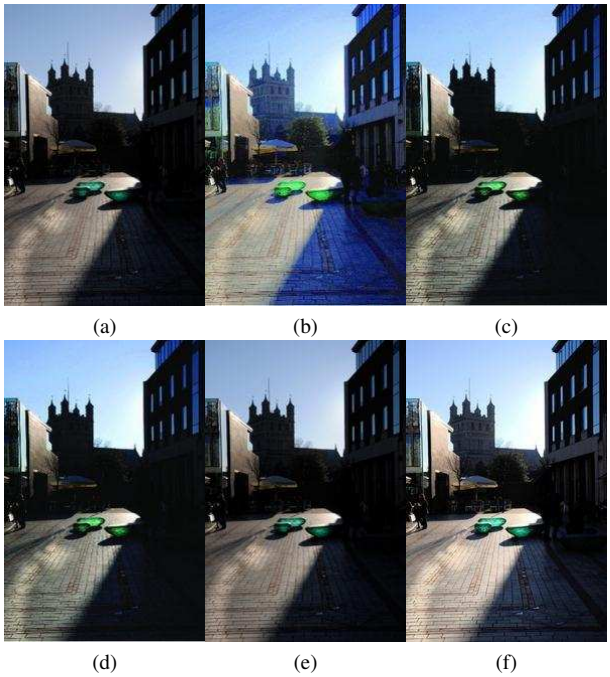

Fig. 10. Dark image: "Street." (a) Original image, (b) HE result, (c) intensity pair result, (d) LRM result, (e) ORMIT result, and (f) proposed method result.

previous research [19], regarding the various possible widths for these regions, supported this equal distribution.

Finally, the enhanced image is a mixture of the region channels; each channel has a different weighting function that emphasizes its characteristics. The final transformation function $\mathscr{T}$ can be computed by

$$\mathscr{T}(i) = \sum_{r=1}^{R} w_r(i) \cdot T_r(i), \tag{13}$$

where w_r is the weighting function for the rth region channel, and $T_r(i)$ indicates the ith position in the rth region channel transformation function. Lastly, the image is enhanced by

$$I_e(x, y) = \mathscr{T}\left(I(x, y)\right), \tag{14}$$

where $I(x, y)$ is the intensity of the pixel (x, y) in the original image, $\mathscr{T}$ is the final transformation function, and I_e is the enhanced image.

In our experiments, each channel has a different weighting function that emphasizes its characteristics. Figure 8a shows three weighting functions for the intensity region channels that emphasize the dark region channel to reduce the dark look of the images. The final weighting functions are shifted Gaussian functions that have been normalized. To construct them, we place their centers in the limits of the intensity range and in the center of the middle region channel. Note that the standard deviation of each Gaussian is proportional to each region in the image. We then normalize the three Gaussian functions so that the contribution of their weights sum to one, as shown in Fig. 8b.

III. Evaluation Framework

Image enhancement is a common procedure. Yet, a simple or standard method to algorithmically assess the quality of an image like a human would does not exist. This type of perceptive contrast measurement is a complex task since several conditions must be considered, such as the state of adaptation of the observer, boundaries between adjacent areas and their relations, the size of the internal structures of the image, and the spatial frequency of the stimuli. Consequently, several contrast models have been introduced to model how the human eye perceives luminance changes, including the Weber law, the power law, and the Michelson law [21].

In addition, several methods have been proposed that attempt to measure the contrast in an image consistently. For example, Gordon and Rangayan [22] proposed a local contrast measure defined by the average of the intensity values detected in two rectangular windows centered on a current pixel. Their method was later improved using the local edge information from the image [23]. Similarly, various measures that quantify contrast block-wise, in which the maximum and minimum intensities inside a block are analyzed to calculate the measure of the enhancement, have been proposed [20], [24], [25]. Unfortunately, these measures are inconsistent because they often fail to reflect the clear improvements in some images, thus scoring it incorrectly. The use of contrast alone is not enough; over-enhanced pictures score high in contrast-based measures, even if their quality is not the best. In response, Morrow *et al*. [26] proposed a measure based on the analysis of the contrast histogram in search of certain characteristics; however, this method was still limited by its emphasis on contrast.

A. Quantitative Measures

To evaluate the image we use three different metrics: measure of enhancement by entropy (EMEE) [25], structural similarity [27], and the newly-proposed metric based on the contrast pairs.

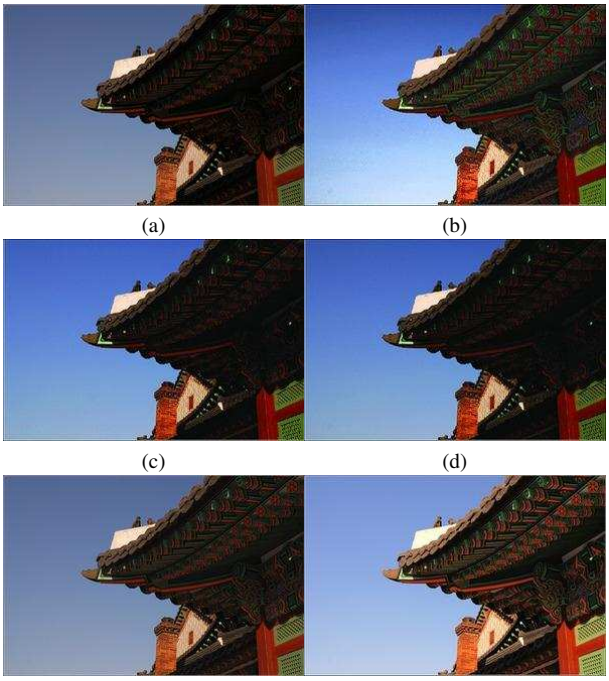

Fig. 11. Dark image: "Building." (a) Original image, (b) HE result, (c) intensity pair result, (d) LRM result, (e) ORMIT result, and (f) proposed method result.

The measure of enhancement by entropy is used to find the average ratio of maximum to minimum intensities in decibels, and it is based upon the concept of entropy [25]. Agaian *et al*. defined the metric as

$$\begin{aligned}\mathrm{EMEE}_{\alpha,k_1,k_2}(I) = \frac{1}{k_1 k_2}\sum_{l=1}^{k_2}\sum_{k=1}^{k_1}\alpha\left(\frac{I_{k,l}^{\max}}{I_{k,l}^{\min}+c}\right)^{\alpha} \\ \times \ln\left(\frac{I_{k,l}^{\max}}{I_{k,l}^{\min}+c}\right),\end{aligned} \tag{15}$$

where the given image I is broken up into $k_1 k_2$ blocks, $I_{k,l}^{\max}$ and $I_{k,l}^{\min}$ are the maximum and minimum intensity in the given (k,l) block, and c is a small constant to avoid division by zero. In our evaluation we used $\alpha = 0.2$, $c = 1$, and a block size of 16×16 pixels.

The structural similarity metric was proposed by Wang *et al*. [27], as an alternative to intensity-based metrics. The structural similarity is based on the assumptions that natural images are highly structured, since their pixels exhibit strong dependencies, and that the human visual system is highly optimized to recover the structural information from an image. Wang *et al*.'s proposed metric is a combination of three components: luminance, contrast, and structure. We estimate the luminance of the image as the mean intensity such that

$$\mu_I = \frac{1}{N}\sum_{x,y} I(x,y), \tag{16}$$

where N is the number of pixels in the image, and $I(x,y)$ is the intensity at the position of the pixel (x,y). Instead of using the correlation proposed by Wang *et al*., we use the ratio of the original image luminance to that of the enhanced

Fig. 12. Dark image: "Subway." (a) Original image, (b) HE result, (c) intensity pair result, (d) LRM result, (e) ORMIT result, and (f) proposed method result.

image. This process allows us to identify the differences in images, given that the enhanced image should be brighter than the original, and simultaneously determine the structural similarities between the images. Note that the definition by Wang *et al*. measures only the similarity to the dark image. Thus, we define the luminance index by the ratio

$$l(I_o, I_e) = \frac{\mu_{I_e}}{\mu_{I_o}}, \tag{17}$$

where I_o is the original image, I_e is the enhanced image, and the means are given by Eq. (16). Wang *et al*. estimate the contrast as the standard deviation of the image, given by

$$\sigma_I = \sqrt{\frac{1}{N-1}\sum_{x,y}(I(x,y)-\mu_I)^2}. \tag{18}$$

Similar to the luminance index, we use the ratio of the contrast of the original image to that of the enhanced image. Hence, the contrast index is defined by

$$c(I_o, I_e) = \frac{\sigma_{I_e}}{\sigma_{I_o}}. \tag{19}$$

Likewise, the structural index is given by the correlation coefficient, which is defined as

$$s(I_o, I_e) = \frac{\sigma_{I_o,I_e} + k}{\sigma_{I_o}\sigma_{I_e} + k}, \tag{20}$$

where k is a constant to avoid division by zero, and σ_{I_o,I_e} is estimated by

$$\sigma_{I_o,I_e} = \frac{1}{N-1}\sum_{x,y}(I_o(x,y)-\mu_{I_o})(I_e(x,y)-\mu_{I_e}), \tag{21}$$

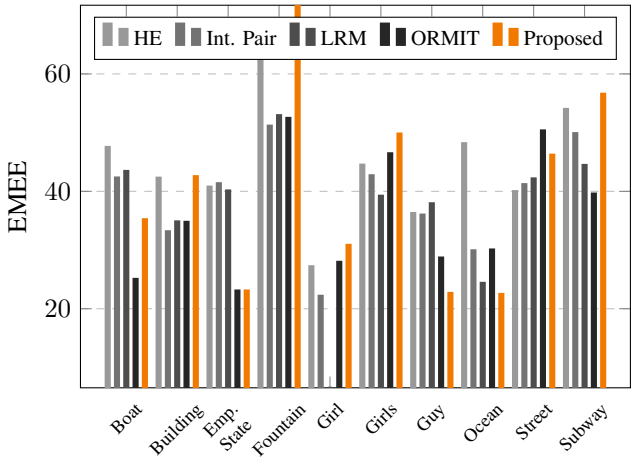

Fig. 13. EMEE (see Eq. (15)) of the results via different methods. The methods with higher values should indicate better quality images; however, this metric does not properly reflect the enhancement of each image.

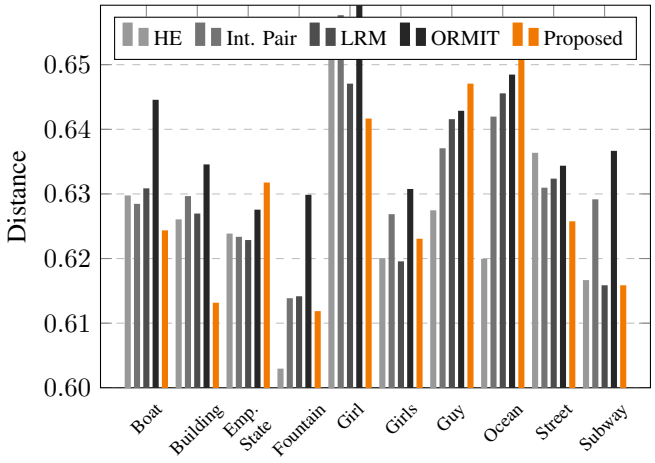

Fig. 14. Distance from the diagonal (see Eq. (26)) of the results via different methods. The methods with smaller distances produce better enhanced images.

where N is the number of pixels of the images, $I_o(x, y)$ and $I_e(x, y)$ are the intensities in the (x, y) position of each image. For our evaluation, we do not mix these indexes as Wang *et al.* proposed. Instead, we analyze them separately, which allows us to do a deeper analysis on the enhancement of each image.

A good enhanced image should have sharp boundaries with smooth regions between the boundaries. To measure these two characteristics, we use the mean of both the edge and the smooth contrast-pair sets. First, we classify the pixels in the image according to the majority of types of contrast pairs it creates, such that

$$\mathbb{E} = \{\rho_i^j \mid |i - j| \geq \varepsilon\}, \tag{22}$$

$$\mathbb{S} = \{\rho_i^j \mid |i - j| < \varepsilon\}, \tag{23}$$

where $\mathbb{E}$ and $\mathbb{S}$ represent the edge and smooth contrast-pair sets, respectively, ρ_i^j is a contrast pair, i and j are the intensities of that contrast pair, and ε is the defined threshold. We then compute the mean of each class using

$$\mu_C = \frac{\sum_{p \in C} p_c}{N_C}, \tag{24}$$

where $C = \{\mathbb{E}, \mathbb{S}\}$ are the contrast-pair classes, μ_C is the mean of class C, p_c is the contrast (intensity difference) of pixel p that belongs to class C, and N_C is the number of pixels in class C. A good enhanced image should have a high edge mean and a small smooth mean, indicating a high contrast change in the boundaries and low contrast change in the flat regions. Consequently, the image can be defined by these two metrics. If we define the images by their two normalized means $I = (\mu_{\mathbb{E}}, \mu_{\mathbb{S}})$, a space $\mathcal{S}$ is formed that holds all the images. The images close to the diagonal, defined by

$$\mu_{\mathbb{E}} + \mu_{\mathbb{S}} - 1 = 0, \tag{25}$$

will have a better appearance. Consequently, by computing the distance between any image $I' = (\mu'_{\mathbb{E}}, \mu'_{\mathbb{S}}) \in \mathcal{S}$ and the diagonal line, we can rank the quality of the images using Eq. (26): The images with the smallest distance present a better enhancement than those farther from the diagonal.

$$D(I') = \frac{\mu'_{\mathbb{E}} + \mu'_{\mathbb{S}} - 1}{\sqrt{2}} \tag{26}$$

B. Qualitative Measures

The enhanced images are for human consumption; therefore, gauging the success of the enhancement based on human opinion is necessary. A subjective measure based on human observation is an effective and reasonable approach. For this study, we asked observers to evaluate the images in four different categories:

- **Similarity:** This characteristic refers to the similarity of the enhanced image compared to the original image. It is used to describe how close the enhanced image is to the original one, while accounting for the potential improvements made to the enhanced image. The question was phrased, "Which enhanced image is most similar to or better than the original?"
- **Edge details:** This characteristic refers to the amount of detail perceived in the enhanced image. It is used to describe how many details the enhancement algorithm preserves and/or reveals from the original image. The question was phrased, "Which enhanced image reveals more of the original image's details?"
- **Color and tonal rendition:** This characteristic refers to any improvements in the colors and tones of the enhanced images with respect to the original. The question was phrased, "Which enhanced image presents better colors and tones with respect to the original?"
- **Artifacts:** This characteristic refers to the robustness of the algorithm against the creation of artifacts. It is used to measure the artifacts created by the enhancement algorithm. The question was phrased, "Which enhanced image presents fewer artifacts?"

For each set of images and for each category, the evaluators were asked to select the result that best exemplified their opinions. They were not informed of the methods that produced each result, and the images were presented in random order. These actions were taken to remove any bias created by viewing previous image sets. We then computed the selection percentage for each method based on the surveyed images chosen by the observers.

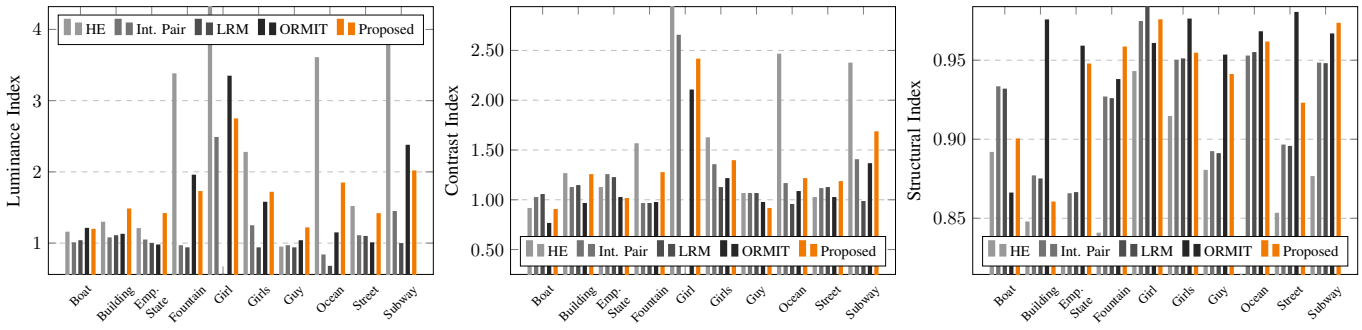

(a) (b) (c)

Fig. 15. Structural similarity indexes of the results from different image enhancement methods: (a) luminance (see Eq. (17)), (b) contrast (see Eq. (19)), and (c) structural (see Eq. (20)). The methods with higher combined indexes produced better images.

IV. Results

In this section, we discuss the performance of the proposed method compared with four alternative methods: histogram equalization (HE), intensity pair algorithm [16], local range modification (LRM) [6], and Orthogonal Retino-Morphic Image Transform (ORMIT) [15]. The HE and LRM methods are known for their ability to reveal the details in dark images. Yet, they cannot enhance mixed images (*i.e.*, those with dark and bright regions), and they produce artifacts in the final image. Similarly, the intensity pair algorithm ineffectively uses the content of the image, producing unnoticeable improvements. The ORMIT, on the other hand, is a widely-used algorithm in consumer electronic devices that provides a good comparison point for demonstrating the superior enhancement capability of the proposed algorithm. To analyze the performances of these algorithms, each method was used to process ten different images in varied locations; all the images were either dark or had shadows. The images included buildings and people, outdoor and indoor scenes, total darkness and mixed light (*i.e.*, dark due to shadows), and close-up and wide depth-of-field images. This large variety of images was employed to validate the superiority of our content-aware algorithm over other methods that are optimized only for certain types of images. Note that we evaluated the images quantitatively and qualitatively.

A. Quantitative Measure

First, we evaluated the methods using the EMEE from Eq. (15). However, this metric does not measure the enhancement as perceived by humans, instead it measures the local contrast variation in each image. For example, the result from HE in "Boat" and "Ocean" images, or from intensity pair in "Emp. State" image (Fig. 16) have a high EMEE value, as shown in Fig. 13, but the enhancement is imperceptible. This effect occurred for other images as well, and in general this metric is not consistent through different images. However, is interesting to note, that the EMEE values, in the "Fountain" image, for HE and for the proposed method are both high, which shows that the proposed method increases the contrast (as much as HE does) and maintains the appearance of the image (something that HE does not). Thus, we used two additional metrics, the structural similarity index and contrast-pair based metric, to evaluate the enhancement. Figure 14 shows the distances of the mean of the enhanced image's contrast-pairs from the diagonal (see Eq. (26)). And Fig. 15 shows the structural similarity indexes of the enhanced images.

Considering our proposed metric, the proposed method scored better in the "Boat," "Building," "Girl," and "Street" images. It revealed details in the shadow areas, as shown in the face of the girl in Fig. 9—an image for which other methods scored poorly in the contrast-pair based metric, and had poor balance in the structural similarity indexes. Additionally, the algorithm was able to maintain the smoothness in the regions of the face and the background. Moreover, ORMIT created strange effects in the skin and in the hair. The proposed algorithm, however, was aware of the texture information in those areas and enhanced them accordingly. Despite the fact that ORMIT had a higher luminance index—due to a wash-out effect—than the proposed method, as shown in Fig. 15a, the contrast index of ORMIT was lower than the proposed method, as shown in Fig. 15b. The structural index, given in Fig. 15c, of both methods was high, indicating that both methods did not introduce errors into the images.

The proposed method was able to recover details in mixed images as well. For example, the "Street" image (Fig. 10) had a shadow due to a building that hid some of the details in the image, but other areas in the image were well-exposed. The proposed method was able to reveal the details near the building and maintain the details in other parts of the image because it created different transformation functions. This behavior is verified in the distance score, and in the balance of the luminance, contrast, and structural indexes—all of which exhibited high scores for the proposed method. The HE result revealed some details in the shadow, but it gave an odd look to the resulting image, as reflected by its structural index. In addition the HE result was over-enhanced, producing a large distance value for the enhanced image, as well as a high luminance index. The other methods produced similar inferior scores with poorly enhanced images.

The proposed method was also able to handle images with complex textures, as shown in the "Building" image (Fig. 11), outperforming the other methods. Both the luminance and contrast index are better than other methods, and it maintained an acceptable structural index. Furthermore, the proposed method

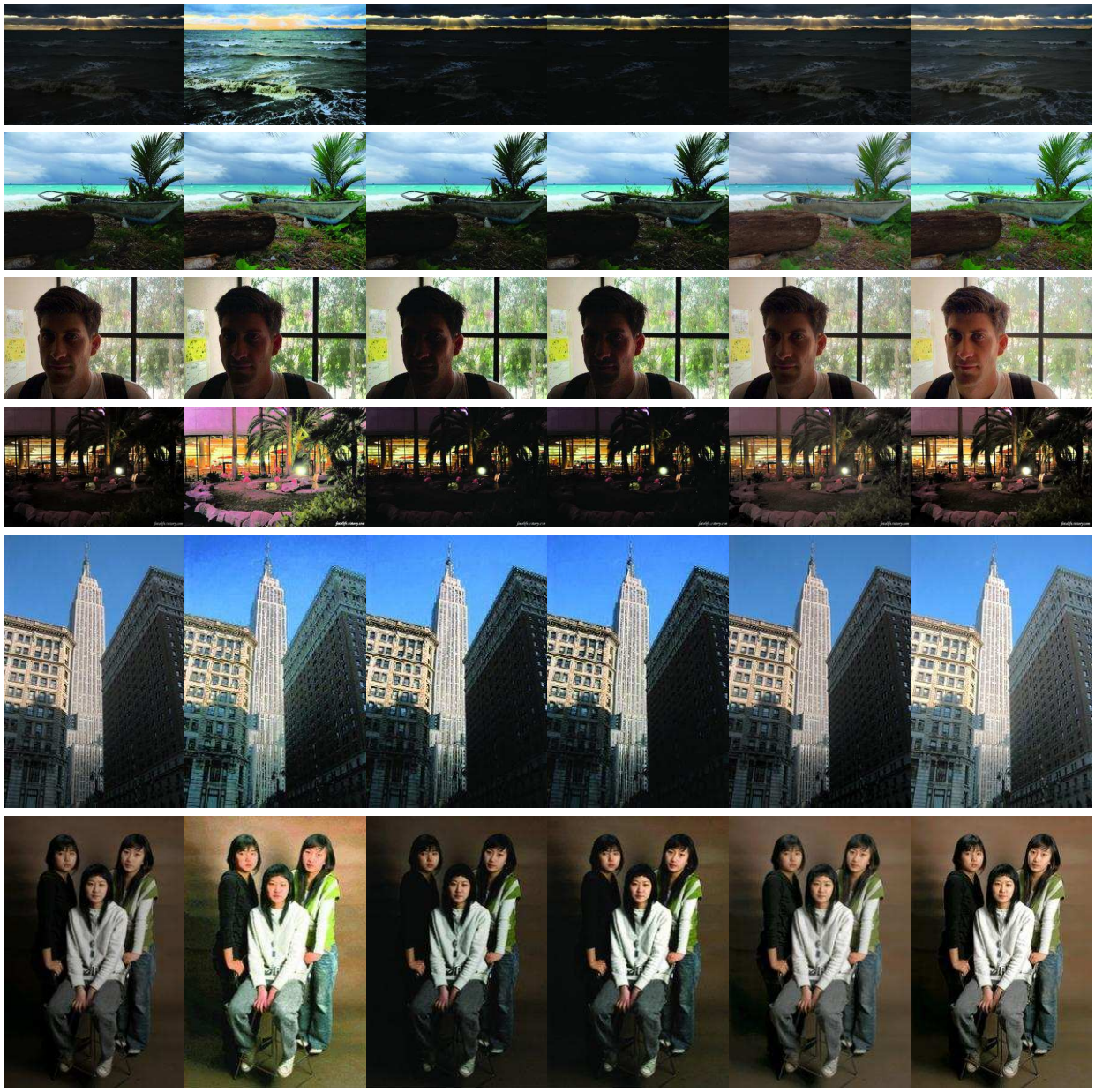

(a) (b) (c) (d) (e) (f)

Fig. 16. Dark images, from top to bottom: "Ocean," "Boat," "Guy," "Fountain," "Empire State," and " Girls." (a) Original image, (b) HE result, (c) intensity pair result, (d) LRM result, (e) ORMIT result, and (f) proposed method result.

revealed details and maintained smoothness in the regions between the textures. This feature can also be appreciated in the "Subway" image (Fig. 12), for which the proposed approach scored better than the other methods, maintained smoothness in the flat regions while revealing the details in the boundaries, and simultaneously increased the brightness of the overall image. These effects are supported by its luminance and contrast indexes, which are not as high as those from the over-enhanced HE result, and by its structural index.

The distances of the other images, however, varied due to enhancement errors. For example, the "Fountain" image (Fig. 16) was over-enhanced by HE, and was darkened by the LRM and intensity pair methods. The over-enhancement gave a false positive in the HE score—the saturated regions resulted in a small contrast mean, while a high contrast in the boundaries was produced. The worst distance score using the proposed method was for the "Ocean" image (Fig. 16). Visually it produced a better result compared to the other methods, but this improvement was not reflected in the contrast-pair metric because the means of the contrast pairs were more compact in the image and had small standard deviation compared to the over-enhanced HE result. The results of the other methods had several edge contrast pairs due to the nearly black tones in the ocean area, thus yielding a better value on the metric. However, the structural similarity index reveals that the proposed method maintained the structure of the image, while producing good luminance and contrast indexes. In general, the structural similarity indexes of ORMIT

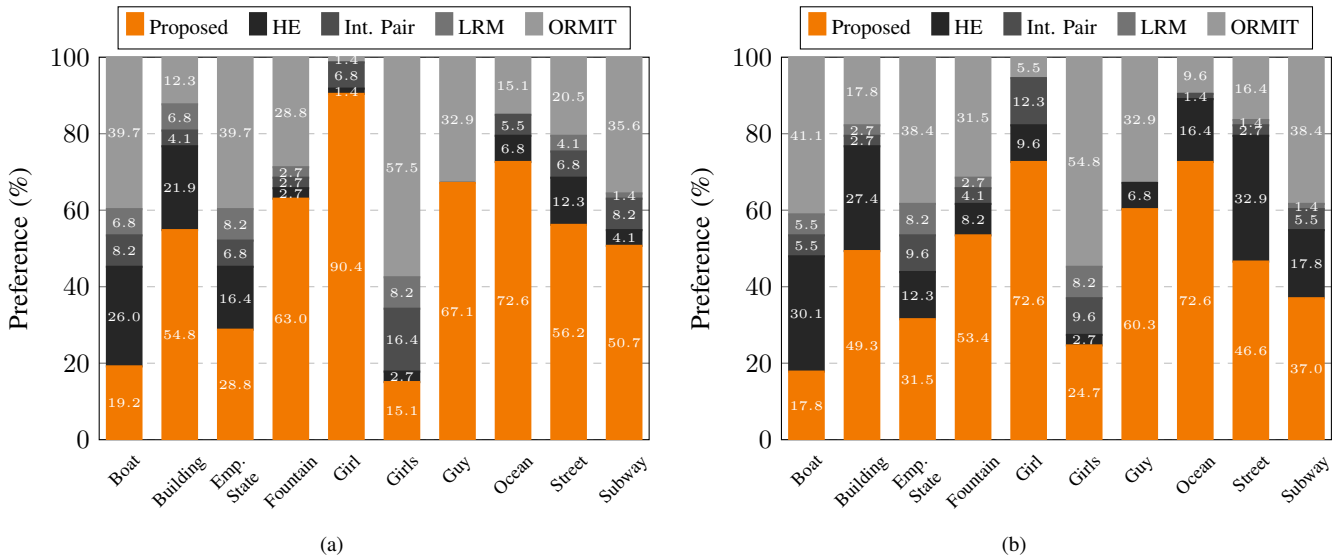

Fig. 17. Percentage of preference for each image according to (a) similarity and (b) edge details.

and the proposed method revealed that they produce the best enhanced images for luminance and contrast, respectively, and simultaneously maintained the structure of the original image.

Overall, the proposed method did a better job at producing images with means closer to ideal images—*i.e.*, points closer to the diagonal in the space defined by the edge and smooth means. Furthermore, the structural similarity indexes reveal that the proposed method procured good luminance and contrast indexes while maintaining the structural index. As Fig. 15 shows, the proposed method maintained the image's structure during the enhancement process and simultaneously increased the luminance and the contrast more than other methods. Moreover, the proposed method out-performed the intensity pair algorithm, which produced sub-par results as revealed by the contrast-pair based metric and the structural similarity indexes. Unfortunately, enhancement errors in the HE results skewed the distance scores, which also introduced peaks in the luminance and contrast indexes, but kept the structural index low in comparison to other methods. Hence, we performed a subjective evaluation of the methods to better assess their performances.

B. Qualitative Measure

Using a survey we qualitatively evaluated 75 people, 57% of which had some knowledge regarding image processing prior to the study. We showed the participants ten different groups of images (Figs. 9–12, 16) consisting of the original image and the results of the different methods (HE, LRM, intensity pair, ORMIT, and the proposed method). They evaluated the results using four different parameters: similarity, edge details, color and tone, and artifacts—as described in Section III-B. We explained the questions to the evaluators in English with additional references for the technical details to ensure that everyone evaluated the images in consistent manner. On average, the proposed method outperformed the other methods in most of the images in all the categories.

The similarity percentages (Fig. 17a) revealed a preference for the proposed method, with the exception of the "Boat," "Emp. State," and "Girls" images, for which the evaluators preferred the ORMIT algorithm. Although the application of the proposed method to the "Boat" image resulted in brighter colors, most of the participants favored the ORMIT result, which had softer colors. The "Emp. State" result from the proposed method was slightly brighter than the ORMIT algorithm; however, 11% more participants chose the ORMIT result. In the "Subway" image, the participants preferred the result of the proposed method, which presented lower enhancement, by more than 15% over the ORMIT result. These findings reveal the variability of personal taste.

The results of the level of edge detail (Fig. 17b) were consistent with the similarity results; the proposed method outperformed other methods in seven of the ten image groups. For the "Subway" image, the increment of the original image's edge details in the ORMIT result was preferred over the proposed method result, but only by a difference of 1.4%. Additionally, the subjective preferences regarding the revealed details for the "Street" image agreed with our quantitative evaluation, as 46% of the participants acknowledged that the proposed method revealed more details than the other methods. This scene was particularly difficult due to the mixture of bright and dark areas in the image. Interestingly, the HE results scored higher in terms of its revealed details than it did in terms of the similarity measure because the participants generally agreed that the HE method produced an improvement in the detail level despite the artifacts and over-enhancement.

In the color and tonal reproduction results (Fig. 18a), the result of the proposed method for the "Boat" image had a lower preference score—probably because the participants considered the brightness increment to be an over-enhancement, and they preferred the color produced by the other methods, such as ORMIT. For the other images, however, the evaluators agreed that the results of the proposed method were the best with the exception of the "Girls" image, for which they preferred the ORMIT result. The colors in the "Emp. State"

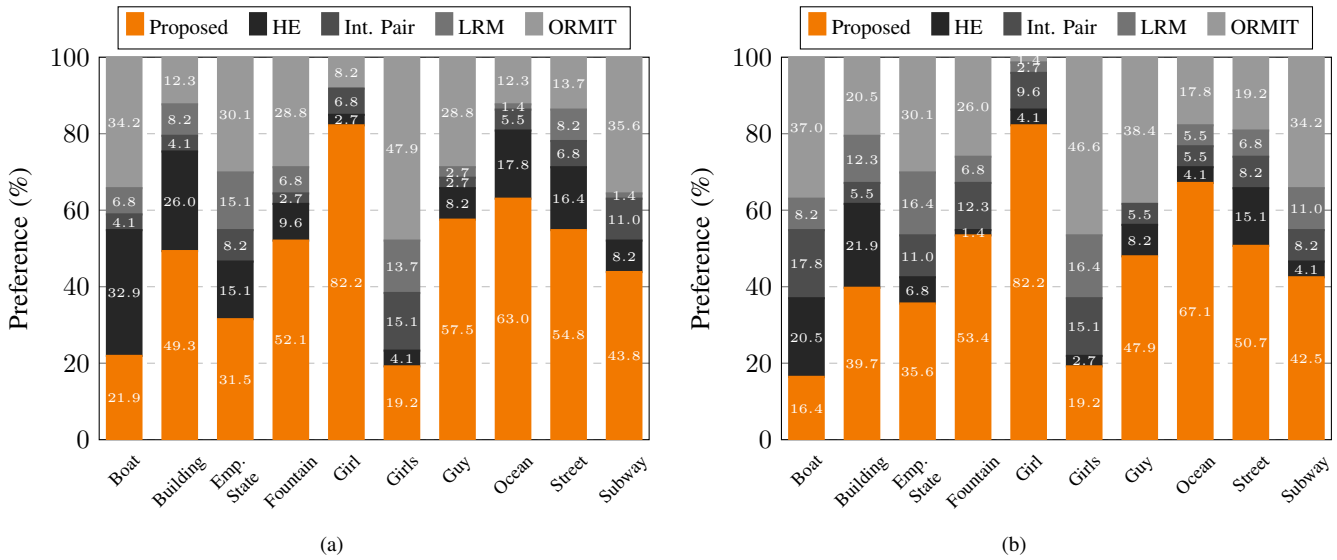

Fig. 18. Percentage of evaluators who preferred each image according to (a) color and tonal rendition and (b) the presence of fewer artifacts.

image generated by the proposed method were preferred over those of ORMIT, despite the evaluators' preference for the ORMIT result in terms of similarity to the original. The color preference results support the robustness of the proposed method, indicating that it preserves the intensities in smooth regions and maintains even colors over large areas, while simultaneously revealing the details in the images.

The evaluators were also asked to select the images with the fewest artifacts (Fig. 18b). In general, the proposed method was the best at reducing the appearance of artifacts. In the "Emp. State" image, the proposed method outperformed the ORMIT algorithm by 5%; however, in the "Girls" and "Boat" images, the ORMIT method had a higher preference rate among the evaluators, of 47% and 37%, respectively. Difficult images such as "Girl," "Fountain," and "Ocean," which were very dark—and thus prone to artifact creation and unnatural appearance—had a high acceptance rate among the evaluators.

In general, image quality is difficult to assess because it depends on human preferences. Even our results that performed poorly according to our quantitative evaluation—such as "Guy" and "Ocean"—were chosen over the results of the other methods in the qualitative evaluation. Likewise, results of the proposed method for images such as "Subway," which did not exhibit as much enhancement as the other methods, were preferred by the evaluators. Ultimately, the individual tastes and backgrounds of the evaluators determined which type of pictures they preferred.

Although the proposed method was able to enhance a wide set of images, it remains limited in certain extreme cases, as shown in Fig. 19. For example, the proposed method cannot recover information from the shadowed or dark areas of images that have near-black intensities. Some parts of the images are still enhanced, but significant amounts of near-black intensities produce undesired effects in the high intensities. Nevertheless, these undesired effects can be minimized by adjusting the weighting functions for the intensity region channels. This adjustment avoids over-enhancement in images with near-black intensities, due to the high accumulation of dark contrast pairs.

V. Conclusion

In the present paper, we introduced a content-aware enhancement algorithm that can improve images from a variety of different environments. The algorithm creates different enhancement functions based on the contents of the image, thereby improving its enhancement capabilities while reducing the artifacts and other unnatural effects in the resulting images. The method analyzes the contents through contrast pairs, which are grouped together according to their intensities. Ideally, this process increases the enhancement and level of detail revealed. Ultimately, the enhancement is intended to mimic the human visual perception, which is accomplished by adaptively combining different region channels. This mixture allows us to enhance some characteristics, such as the details in dark and bright regions, while preserving others, such as the tones in smooth and flat regions.

The proposed method is robust because it adapts its transformation functions to the contents of the image, which avoids the introduction of errors in the image. The mixture of different region channels also increases the quality of the output because it allows a distinct enhancement for different parts of the image. This process avoids over-enhancement problems in areas with normal dynamic ranges.

References

[1] R. C. Gonzalez and R. E. Woods, *Digital Image Processing (3rd Edition)*. Upper Saddle River, NJ, USA: Prentice-Hall, Inc., 2006.

[2] Y.-T. Kim, "Contrast enhancement using brightness preserving bi-histogram equalization," *IEEE Trans. Consum. Electron.*, vol. 43, no. 1, pp. 1–8, 1997.

[3] T. K. Kim, J. K. Paik, and B. S. Kang, "Contrast enhancement system using spatially adaptive histogram equalization with temporal filtering," *IEEE Trans. Consum. Electron.*, vol. 44, no. 1, pp. 82 –87, Feb. 1998.

[4] J.-Y. Kim, L.-S. Kim, and S.-H. Hwang, "An advanced contrast enhancement using partially overlapped sub-block histogram equalization," *IEEE Trans. Circuits Syst. Video Technol.*, vol. 11, no. 4, pp. 475 –484, Apr. 2001.

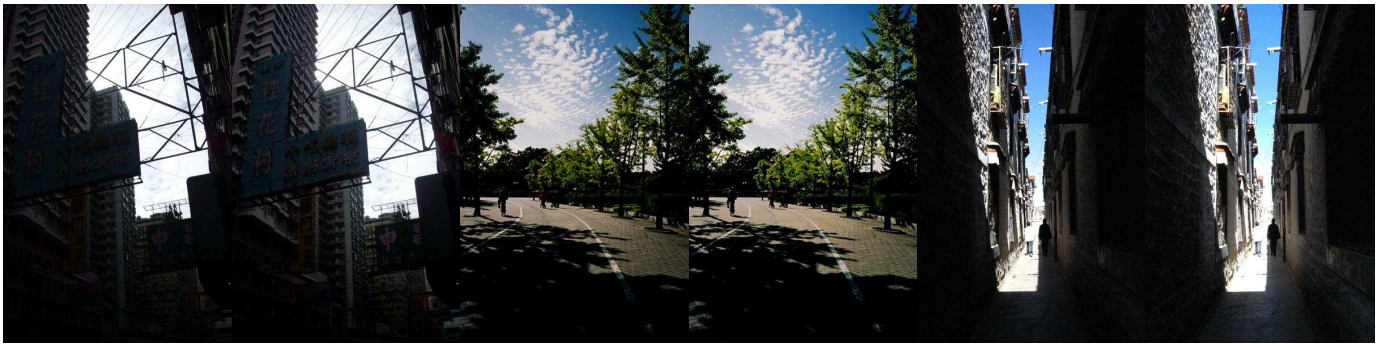

(a) (b) (c) (d) (e) (f)

Fig. 19. Images with near-black intensities are not fully enhanced by the proposed algorithm: (a), (c), and (e) show original images, while (b), (d), and (f) show results of the proposed algorithm.

[5] K. Wongsritong, K. Kittayaruasiriwat, F. Cheevasuvit, K. Dejhan, and A. Somboonkaew, "Contrast enhancement using multipeak histogram equalization with brightness preserving," in *Circuits and Systems, 1998. IEEE APCCAS 1998. The 1998 IEEE Asia-Pacific Conference on*, Nov. 1998, pp. 455 –458.

[6] J. D. Fahnestock and R. A. Schowengerdt, "Spatially Variant contrast enhancement using local range modification," *Optical Engineering*, vol. 22, no. 3, pp. 378–381, 1983.

[7] I. Safonov, M. Rychagov, K. Kang, and S. H. Kim, "Automatic correction of exposure problems in photo printer," in *Consumer Electronics, 2006. ISCE '06. 2006 IEEE Tenth International Symposium on*, 0-0 2006, pp. 1 –6.

[8] D. J. Jobson, Z. ur Rahman, and G. A. Woodell, "A multiscale retinex for bridging the gap between color images and the human observation of scenes," *IEEE Trans. Image Process.*, vol. 6, no. 7, pp. 965–976, 1997.

[9] E. H. Land, "An Alternative Technique for the Computation of the Designator in the Retinex Theory of Color Vision," *PNAS*, vol. 83, no. 10, pp. 3078–3080, May 1986. [Online]. Available: http://dx.doi.org/10.1073/pnas.83.10.3078

[10] E. H. Land and J. J. McCann, "Lightness and Retinex Theory," *J. Opt. Soc. Am.*, vol. 61, no. 1, pp. 1–11, Jan. 1971. [Online]. Available: http://www.opticsinfobase.org/abstract.cfm?URI=josa-61-1-1

[11] G. Orsini, G. Ramponi, P. Carrai, and R. Di Federico, "A modified retinex for image contrast enhancement and dynamics control," in *Image Processing, 2003. ICIP 2003. Proceedings. 2003 International Conference on*, vol. 3, Sep. 2003, pp. III – 393–6 vol.2.

[12] R. Sobol, "Improving the Retinex algorithm for rendering wide dynamic range photographs," *Journal of Electronic Imaging*, vol. 13, no. 1, pp. 65–74, 2004.

[13] L. Tao and V. Asari, "Modified luminance based msr for fast and efficient image enhancement," in *Applied Imagery Pattern Recognition Workshop, 2003. Proceedings. 32nd*, Oct. 2003, pp. 174 – 179.

[14] T. Watanabe, Y. Kuwahara, A. Kojima, and T. Kurosawa, "An adaptive multi-scale retinex algorithm realizing high color quality and high-speed processing," *Journal of imaging science and technology*, vol. 49, 2005.

[15] V. Chesnokov, "Image enhancement methods and apparatus therefor," Unated States Patent 7302110, 2002.

[16] T.-C. Jen, B. Hsieh, and S.-J. Wang, "Image contrast enhancement based on intensity-pair distribution," in *Image Processing, 2005. ICIP 2005. IEEE International Conference on*, vol. 1, Sep. 2005, pp. I – 913–16.

[17] R. Bilcu and M. Vehvilainen, "Robust intensity-pair distribution for image contrast enhancement," in *Multimedia and Expo, 2007 IEEE International Conference on*, Jul. 2007, pp. 1627 –1630.

[18] N.-C. Wang and S.-C. Tai, "Automatic intensity-pair distribution for image contrast enhancement," in *Communications, Control and Signal Processing, 2008. ISCCSP 2008. 3rd International Symposium on*, Mar. 2008, pp. 566 –571.

[19] M. K. Kundu and S. K. Pal, "Thresholding for edge detection using human psychovisual phenomena," *Pattern Recogn. Lett.*, vol. 4, pp. 433–441, Dec. 1986. [Online]. Available: http://dl.acm.org/citation.cfm?id=20751.20755

[20] K. Panetta, E. Wharton, and S. Agaian, "Human visual system-based image enhancement and logarithmic contrast measure," *IEEE Trans. Syst., Man, Cybern. B*, vol. 38, no. 1, pp. 174 –188, Feb. 2008.

[21] A. K. Jain, *Fundamentals of digital image processing*. Upper Saddle River, NJ, USA: Prentice-Hall, Inc., 1989.

[22] R. Gordon and R. M. Rangayyan, "Feature enhancement of film mammograms using fixed and adaptive neighborhoods," *Appl. Opt.*, vol. 23, no. 4, pp. 560–564, Feb. 1984.

[23] A. Beghdadi and A. le Negrate, "Contrast enhancement technique based on local detection of edges," *Comput. Vision Graph. Image Process.*, vol. 46, pp. 162–174, May 1989.

[24] S. Agaian, K. Panetta, and A. Grigoryan, "Transform-based image enhancement algorithms with performance measure," *IEEE Trans. Image Process.*, vol. 10, no. 3, pp. 367 –382, Mar. 2001.

[25] S. Agaian, B. Silver, and K. Panetta, "Transform coefficient histogram-based image enhancement algorithms using contrast entropy," *IEEE Trans. Image Process.*, vol. 16, no. 3, pp. 741 –758, Mar. 2007.

[26] W. Morrow, R. Paranjape, R. Rangayyan, and J. Desautels, "Region-based contrast enhancement of mammograms," *IEEE Trans. Med. Imag.*, vol. 11, no. 3, pp. 392 –406, Sep. 1992.

[27] Z. Wang, A. Bovik, H. Sheikh, and E. Simoncelli, "Image quality assessment: from error visibility to structural similarity," *IEEE Trans. Image Process.*, vol. 13, no. 4, pp. 600 –612, Apr. 2004.

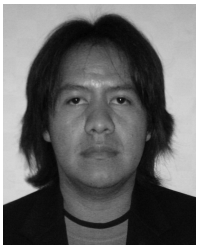

Adin Ramirez Rivera received his BSc degree in Computer Engineering from San Carlos University (USAC), Guatemala in 2009. He is currently working towards his PhD degree in the Department of Computer Engineering, Kyung Hee University, South Korea. His research interests are image enhancement, object detection, expression recognition, and pattern recognition.

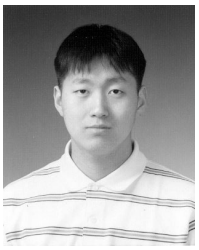

Byungyong Ryu received his BSc degree in Computer Engineering from Kyung Hee University, South Korea, in 2010. He is currently working towards his PhD degree in the Department of Computer Engineering, Kyung Hee University, South Korea. His research interests are image enhancement, and medical image processing in dentistry.

Oksam Chae received his BSc degree in Electronics Engineering from Inha University, South Korea in 1977. He completed his M.S. and Ph.D. degree in Electrical and Computer Engineering from Oklahoma State University, USA in 1982 and 1986, respectively. From 1986 to 88, he worked as a research engineer in Texas Instruments Image Processing Laboratory, USA. From 1988, he has been working as a professor in the Department of Computer Engineering, Kyung Hee University, South Korea. His research interest includes multimedia data processing environment, intrusion detection system, sensor networks and medical image processing in dentistry. He is a member of IEEE, SPIE, KES and IEICE.